THE JOURNAL OF PHYSICAL CHEMISTRY Letters

Perspective

pubs.acs.org/JPCL

Formation of Low-Volatility Organic Compounds in the Atmosphere: Recent Advancements and Insights

Kelley C. Barsanti,*[,†] Jesse H. Kroll,[‡] and Joel A. Thornton[§]

[†]Chemical and Environmental Engineering, Center for Environmental Research and Technology, University of California-Riverside, Riverside, California 92521, United States

[‡]Civil and Environmental Engineering, Chemical Engineering, Massachusetts Institute of Technology, Cambridge, Massachusetts 02139, United States

[§]Atmospheric Sciences, University of Washington, Seattle, Washington 98195, United States

ABSTRACT: Secondary organic aerosol (SOA) formation proceeds by bimolecular gas-phase oxidation reactions generating species that are sufficiently low in volatility to partition into the condensed phase. Advances in instrumentation have revealed that atmospheric SOA is less volatile and more oxidized than can be explained solely by these well-studied gas-phase oxidation pathways, supporting the role of additional chemical processes. These processes—autoxidation, accretion, and organic salt formation—can lead to exceedingly low-volatility species that recently have been identified in laboratory and field studies. Despite these new insights, the identities of the condensing species at the molecular level and the relative importance of the various formation processes remain poorly constrained. The thermodynamics of autoxidation, accretion, and organic salt formation can be described by equilibrium partitioning theory; a framework for which is presented here. This framework will facilitate the inclusion of such processes in model representations of SOA formation.

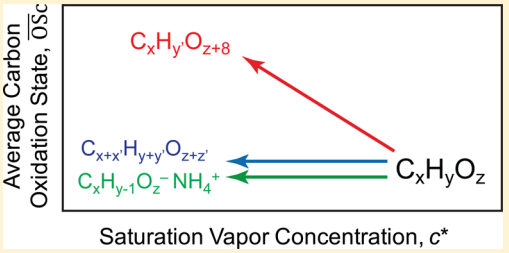

The fate and transport of organic compounds in the atmosphere are highly influenced by phase. Gas-phase organic compounds are subject to free radical oxidation (e.g., by ozone (O_3), hydroxyl radical (OH), and nitrate radical (NO_3)), which results in fragmentation and functionalization. The thermodynamic end point of fragmentation is conversion into carbon dioxide. Functionalization decreases the volatility of gas-phase organic compounds, allowing partitioning from the gas to the condensed phase. In the atmosphere, condensed-phase organic matter is in the form of suspended particles with sizes ranging from 10 to 10^4 nm, commonly referred to as organic aerosol (OA). OA is further categorized as either condensable compounds that are directly emitted (primary OA, or POA) or those that are formed in situ following chemical change (secondary OA, or SOA). While the lifetime of OA is on the order of days to weeks, OA is dynamic and the phase distribution and lifetimes of individual organic compounds depend on the relative time scales of reaction and partitioning.[1,2] Oxidation time scales in the particle phase are long relative to the gas phase, and evaporation time scales may be long relative to oxidation at the particle surface. Thus OA may act as a relatively long-lived intermediate in the oxidation of atmospheric organic species.[3] In addition to importance in the lifecycle of organic carbon, OA makes up a major mass fraction of submicron aerosol mass and therefore adversely affects air quality and alters the Earth's radiative budget.

Equilibrium gas-particle partitioning theory has been widely used to model the extent to which compounds are present in the gas versus the condensed (particle) phase.[4,5] On the basis of partitioning theory, the gas-particle partitioning constant of an individual compound ($K_{p,i}$) can be represented as follows

$$K_{p,i} = \frac{[i_p]/M_{OA}}{[i_g]} = \frac{RT}{10^6 \overline{MW}_{OA} \zeta_i p^\circ_{L,i}} \quad (1)$$

where $[i_p]$ is the mass concentration of i in the condensed phase, M_{OA} is the mass concentration of the condensed phase (for a pure organic phase), $[i_g]$ is the mass concentration of i in the gas phase, R is the ideal gas constant, T is temperature, $\overline{MW}_{OA}$ is the average molecular weight (MW) of the condensed organic phase, ξ_i is the mole-scale activity coefficient of i in the condensed phase, and $p^\circ_{L,i}$ is the subcooled pure-liquid vapor pressure of i. It can be advantageous to represent K_p ($m^3\ \mu g^{-1}$) in inverse units, as the saturation vapor concentration (c^* in units of $\mu g\ m^{-3}$).[6] Equation 1 can be applied when the condensed phase includes inorganic compounds and water, as is typical in atmospheric particles, by replacing M_{OA} and $\overline{MW}_{OA}$ with M_{TPM} and $\overline{MW}_{TPM}$, respectively (where TPM = total particulate matter).[7,8] The accuracy of the predictions depends on how well the identities and properties of the partitioning compounds are known and how well they are represented (i.e., as individual compounds or lumped surrogates).

Received: December 17, 2016
Accepted: March 10, 2017
Published: March 10, 2017

DOI: 10.1021/acs.jpclett.6b02969
J. Phys. Chem. Lett. 2017, 8, 1503−1511

A major consideration in the application of eq 1 is whether the assumption of gas-particle equilibrium is valid across atmospherically relevant particle sizes and conditions (e.g., relative humidity (RH) and T). Recent studies have demonstrated that the equilibrium assumption does not always hold;[9,10] in particular, when the effective bulk diffusivity of an organic compound is $< \sim 10^{-15}$ cm^2 s^{-1}, gas-particle equilibration can take several hours or even days.[9] For particles in the atmosphere the consideration of nonequilibrium partitioning may be most important for semivolatile organic compounds (10^{-1} μg m^{-3} $< c^* < 10^2$ μg m^{-3}) at lower RH (<30%).[11] For such cases a kinetic representation of partitioning may be required. Deviations between measured and predicted partitioning do not indicate an inherent failure in partitioning theory but rather that: (1) equilibrium has not been achieved at the time of measurement; (2) the properties of condensing compounds or the particle phase (e.g., volatilities, activity coefficients) are not adequately known; or (3) condensed-phase low-volatility compounds are significantly altered during sampling and analysis.

Extended modeling approaches, as well as advances in instrumentation used to detect gas- and particle-phase organic compounds and to probe the chemical and physical properties of SOA, have led to new insights into the formation of (E)LVOCs in the atmosphere.

According to eq 1, at atmospherically relevant OA concentrations of 1−10 μg m^{-3}, c_i^* values <100 μg m^{-3} ($p^\circ_{L,i}$ $< \sim 10^{-8}$ atm) are required for compound i to be present (>1%) in the condensed phase. A large pool of gas-phase organic compounds, $c^* > 100$ μg m^{-3}, serves as precursors for the lower volatility compounds that condense to form SOA. A key challenge in the field of atmospheric chemistry is to determine both the amount of the volatile organic compound (VOC) pool that is transformed into the lesser-abundant low-volatility components of SOA and the chemical processes by which VOCs are converted. The distribution of atmospheric organic carbon mass among different compounds with varying volatility and their formation processes are not generally known; this includes the extent to which the volatility distribution is controlled by functionalization and fragmentation during gas-phase free radical oxidation and by multiphase reactions involving radical and closed-shell compounds. Closed-shell reactions include accretion reactions, in which two or more compounds react to form higher molecular weight and lower volatility products,[12] and organic salt formation. With organic salt formation, the ionized fractions of organic acids or bases are effectively nonvolatile and thus exist entirely in the condensed phase,[7] whereas the neutral species typically are too volatile to contribute appreciably to SOA. The formation of condensed-phase accretion products and organic salts shifts the equilibrium of the partitioning compounds, further promoting gas-to-particle conversion.[7] Accretion and organic salt formation may occur in the gas phase, although significant kinetic limitations likely exist. Representative oxidation and accretion reactions and resultant decreases in volatility and changes in oxidation state are illustrated in Figure 1.

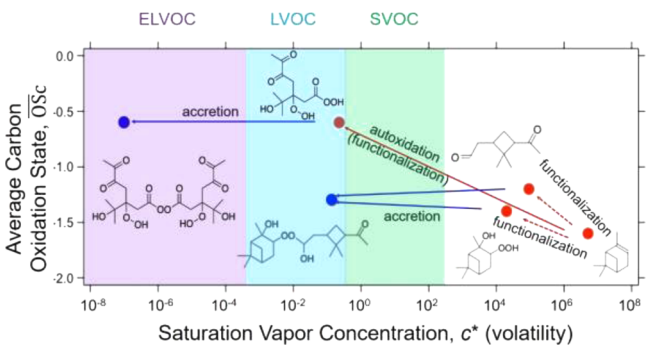

Figure 1. Two-dimensional volatility basis set representation of atmospherically relevant organic molecules, showing their approximate average carbon oxidation state ($\overline{OS}_C$) and saturation vapor concentration (c^*, log scale). Volatility decreases from right to left on the x axis; under ambient conditions semivolatile organic compounds (SVOCs) are partitioned between the gas and particle phases, and low-volatility and extremely low-volatility organic compounds (LVOCs and ELVOCs, respectively) exist largely to entirely in the particle phase. Volatile organic compounds undergo gas-phase oxidation resulting in fragmentation (not shown) and functionalization. Stepwise functionalization may lead to the addition of a few oxygen atoms, while autoxidation leads to highly oxygenated and low volatility organic molecules. Accretion reactions between organic compounds also lead to low-volatility molecules.

Multifunctional oxidation and accretion product formation have been reviewed previously in the context of atmospheric SOA by Hallquist et al.,[13] Kroll and Seinfeld,[3] and Ziemann and Atkinson.[14] This Perspective highlights recent advances in our understanding of the formation and persistence of low-volatility and extremely low-volatility organic compounds ((E)LVOCs) in both the gas and particle phases. These subclasses of organic compounds are defined as having 10^{-4} μg m^{-3} $< c^* < 10^{-1}$ μg m^{-3} ($p^\circ_L \approx 10^{-11}$ to 10^{-14} atm) and $c^* < 10^{-4}$ μg m^{-3} ($p^\circ_L < \sim 10^{-14}$ atm), respectively[15] (see Figure 1). As such, these classes will preferentially exist (>90%) in the particle phase under all ambient conditions, and thus even small sources of such compounds may contribute significantly to SOA. Extended modeling approaches, as well as advances in instrumentation used to detect gas- and particle-phase organic compounds and to probe the chemical and physical properties of SOA, have led to new insights into the formation of (E)LVOCs in the atmosphere. This Perspective is focused on three such insights: (1) gas-phase radical oxidation produces multifunctional low-volatility products much more promptly than previously expected; (2) multiphase chemistry that can lead to accretion of organic compounds into oligomeric products is common and significant; and (3) acid−base chemistry and other organic−inorganic interactions can lead to effectively nonvolatile organic matter. Gas-particle partitioning theory is used here to provide a framework for considering the potential contributions of (E)LVOCs to SOA formation and to facilitate the inclusion of these non-negligible pathways in current and future model representations of SOA.

The prevailing view of SOA formation has been that the functionalization of gas-phase organic compounds occurs in a stepwise sequential manner, wherein reaction between a closed-shell organic precursor and oxidant such as O_3, OH, or NO_3

DOI: 10.1021/acs.jpclett.6b02969
J. Phys. Chem. Lett. 2017, 8, 1503−1511

leads to, on average, the addition of one to two functional groups (e.g., a carbonyl, hydroperoxide, hydroxy, or nitrate group, etc.). Via these standard reaction channels, the single-step oxidation of the C10 hydrocarbon α-pinene may add only one to four oxygen atoms. The requirement of a reaction between oxidant and VOC introduces thermodynamic and kinetic limitations on the formation of SOA from reduced hydrocarbon precursors. In the well-mixed planetary boundary layer, this limitation affects the total pool of condensable vapors because each functionalized oxidation product that remains in the gas phase is subject to losses by deposition, photolysis, and fragmentation in competition with further functionalization.

Recent theoretical and observational studies of gas-phase oxidation have shown that this stepwise functionalization pathway can be short-circuited by intramolecular reactions of the organic peroxy radical (RO_2) intermediates typically formed upon reaction of the VOC and oxidant. In short, the RO_2 radical undergoes intramolecular H-atom abstraction reactions, allowing rapid autoxidation.

Recent theoretical and observational studies of gas-phase oxidation have shown that this stepwise functionalization pathway can be short-circuited by intramolecular reactions of the organic peroxy radical (RO_2) intermediates typically formed upon reaction of the VOC and oxidant. In short, the RO_2 radical undergoes intramolecular H-atom abstraction reactions, allowing rapid autoxidation. Autoxidation proceeds when the peroxy moiety abstracts an H from another C on the molecule to create a hydroperoxide functionality and a new radical center, to which O_2 adds, leading to a new peroxy radical moiety. The process can then repeat several times, adding hydroperoxide functional groups and ultimately terminating by either uni- or bimolecular pathways (Figure 2). Observational and theoretical estimates suggest that some H-abstraction steps can occur on the 0.1 to 1 s^{-1} time scale.[16] For comparison, the frequency of RO_2 bimolecular reactions with HO_2 is on the order of 0.01 s^{-1}, implying that a distribution of highly oxygenated RO_2 and even the corresponding closed-shell products of the autoxidation pathway are established nearly instantaneously.[17−20]

This class of "autoxidation" reaction has long been known to be an important channel for RO_2 radicals in high-temperature combustion[21,22] and food spoiling,[23] but was previously thought not to be important in atmospheric organic chemistry due to the large barrier heights involved in the initial steps of hydrocarbon oxidation. However, such barriers are now known to be substantially lower for functionalized RO_2 radicals due to the weakening of the C−H bond by adjacent oxygen-containing functional groups, enabling such H-transfer reactions to occur rapidly at near room temperature. This pathway was first shown to be important under ambient conditions in the oxidation of isoprene.[17,24,25] First-generation isoprene-derived RO_2 radicals

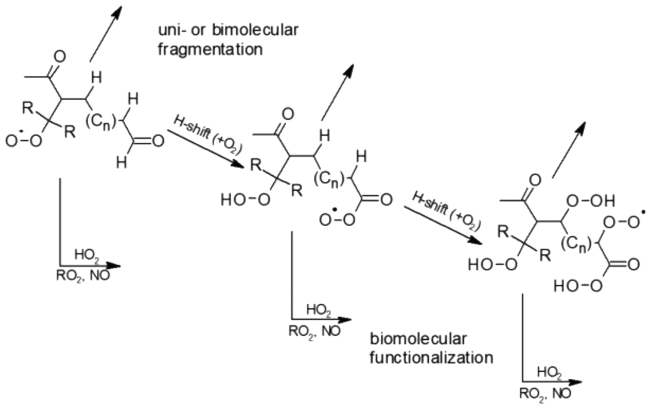

Figure 2. Schematic of autoxidation by intramolecular RO_2 radical H atom abstraction. The peroxy moiety abstracts an H from another C to create a hydroperoxide functionality and a new radical center, to which O_2 adds, leading to a new peroxy radical moiety. This can repeat several times, adding hydroperoxide functional groups and ultimately terminating by either a uni- or bimolecular pathway.

can undergo a unimolecular 1−6 H-shift to yield a hydroperoxyenal at rates as high as 0.3 s^{-1} and ∼0.002 s^{-1} for an isomer-weighted rate coefficient.[17,26] Related RO_2 intramolecular H atom abstractions throughout the isoprene and monoterpene oxidation mechanisms now have been proposed.[18,20,26−28] While energy barriers estimated for some of the likely H-abstraction steps are lower than expected for nonfunctionalized RO_2, the barriers are not insignificant. Thus a strong temperature dependence to the autoxidation process is expected, which would therefore influence its importance relative to bimolecular reactions in the atmosphere.

RO_2 isomerization reactions, particularly when occurring multiple times in sequence, can rapidly lower the vapor pressures of organic species by adding multiple functional groups to the carbon skeleton. The role of such reactions in lowering vapor pressure for a range of molecules was demonstrated by Crounse et al.[23] and Ehn et al.[27] Ehn et al., using a high-resolution time-of-flight (nitrate adduct) chemical ionization mass spectrometer (HR-ToF-CIMS),[29] showed that ozonolysis of α-pinene, and endocyclic alkenes generally, promptly led to the formation of highly oxygenated and very low-volatility RO_2 and closed-shell products in the gas phase. In the case of α-pinene, RO_2 radicals with compositions of $C_{10}H_{15}O_{8-12}$ were observed, as were corresponding "monomer" and "dimer" closed-shell products having compositions of $C_{9-10}H_{14-16}O_{8-12}$ and $C_{18-20}H_{28-32}O_{16-24}$. The response of these highly oxygenated (E)LVOC products to variations under oxidation conditions is consistent with a fraction of the RO_2 radicals, produced upon decomposition of the Criegee radical, undergoing a multistep intramolecular autoxidation process.

On the basis of estimated vapor pressures, the autoxidation products are (E)LVOCs and thus would exist largely in the particle phase. Indeed, major contributions of these (E)LVOCs to SOA were demonstrated during laboratory experiments by Ehn et al.[18] and Trostl et al.[30] The gas-phase molar yields of these highly oxygenated (E)LVOCs are surprisingly large, estimated at 3.5−6.5% (with a relative uncertainty of ∼±50%);[18,28] thus such reaction products can by themselves account for a substantial fraction of the SOA production in these experiments. However, because most previous SOA laboratory studies were run under conditions in which RO_2 radicals reacted with HO_2 or other RO_2 radicals rather than

DOI: 10.1021/acs.jpclett.6b02969
J. Phys. Chem. Lett. 2017, 8, 1503−1511

isomerized, it is difficult to compare the SOA yields measured in Ehn et al.[18] and Trostl et al.[30] with those from previous studies. This highlights the need for future laboratory experiments that simulate the range of atmospheric lifetimes of large RO_2 radicals (e.g., one to hundreds of seconds under pristine conditions).

The fact that gas-phase autoxidation products are detected as dimers suggests that gas-phase accretion reactions may occur in parallel with autoxidation, wherein RO_2 radicals serve as the reacting monomers. RO_2 radicals and Criegee intermediates previously have been identified as potential monomers in accretion pathways, along with closed-shell stable monomers.[31] Some of the first evidence of E(LVOC) formation by accretion reactions was provided by Tobias and Ziemann,[32,33] who used temperature-programmed desorption to demonstrate that within laboratory-generated SOA some components evaporate at temperatures higher than expected based on their physical volatility alone. This behavior was explained by the particle-phase reaction of aldehydes with hydroperoxides to form peroxyhemiacetal accretion products; upon heating, such products will then thermally decompose back to aldehydes and hydroperoxides. Jang and Kamens[34] also suggested that reversible accretion reactions (e.g., hemiacetal/acetal formation and aldol condensation) could explain the large measured K_p values for relatively volatile organic compounds. Discrepancies between measured and calculated volatility also have been demonstrated recently using advanced instrumentation (HR-ToF-CIMS[35] and semivolatile thermal desorption aerosol gas (SV-TAG) chromatography[36,37]) for compound identification, providing further indirect evidence of decomposition of accretion products prior to analysis.

Direct evidence of the formation of accretion products comes from chemical analysis of OA particles. This includes online studies in which dimers and trimers were detected directly.[35,38,39] However, most such evidence comes from offline analyses in which particles are collected onto filters and analyzed using techniques that minimize heating (e.g., electrospray ionization). Accretion products were first detected using offline techniques in laboratory-generated SOA by Tolocka et al.[40] and by Kalberer et al.,[41] and have since been observed in a number of chemical systems using a range of techniques (e.g., ref 42). Theoretical studies have further supported the role of accretion reactions in forming SOA,[43−45] while also illustrating that some reactions are more thermodynamically feasible than others. A computational chemistry study by DePalma et al.[45] demonstrated that peroxyhemiacetal formation and aldol addition are among the most thermodynamically favorable accretion reactions forming covalently bound organic compounds (Gibbs free energies in Table 1). Considering the kinetics of accretion product formation, Ziemann and Atkinson[14] concluded that for atmospherically relevant time scales in clean environments peroxyhemiacetals and esters are the most likely accretion products, and under polluted conditions, hemiacetals likely are dominant (reaction rate constants in Table 1).

In addition to organic constituents, atmospheric particles typically contain significant fractions of inorganic compounds and water. Such constituents promote organic salt formation and accretion reactions in which inorganic compounds serve as monomers or catalysts. In 2001, Angelino et al.[46] identified short-chain alkylamines in ambient particles using a single-particle mass spectrometer. Laboratory experiments were used to confirm that organic salt formation (alkylamines + nitrate or

Table 1. Reported Gibbs Free Energies (ΔG_f°) and Reaction Rate Constants (k) for Selected Accretion Reactions[a]

	gas phase (kJ mol^{-1} @ 298 K)	aqueous phase (kJ mol^{-1} @ 298 K)	methanol (kJ mol^{-1} @ 298 K)	aqueous-phase rate constant (k)	methanol rate constant (k)	"other" solvents rate constant (k)
acid dimer (homodimer)	−27.0 to −33.3	−9.09 to −37.5	−6.91 to −31.8			
acid dimer (heterodimer)	−29.1 to −30.4	18.4	26.9 to −3.68			
peroxyhemiacetal	−14.5	−4.54	−1.03			0.5 to 70 M^{-1} h^{-1}
hemiacetal	32.9	34.2		*3.2 × 10^3 M^{-2} h^{-1}	*4.9 × 10^6 M^{-2} h^{-1}	
acetal				*1.6 × 10^2 M^{-2} h^{-1}	*2.9 × 10^3 M^{-2} h^{-1}	
esterification	27.2	15.9			*6.5 to 110 M^{-2} h^{-1}	
amide formation						
aldol addition	9.76	−4.07	0.59			*7.2 × 10^{-3} M^{-2} h^{-1}

[a]Gibbs free energies from DePalma et al.[45] for specific molecular structures; reaction rate constants from Ziemann and Atkinson[14] for diverse molecular structures. *Indicates H+ conditions, under which rate constants are dependent on the acid concentration and thus are third-order. Reported hemiacetal values under acetic (acetic acid) conditions: 3.5 M^{-2} h^{-1} (aq) and 26 M^{-2} h^{-1} (MeOH) and hemiacetal under neutral conditions (second order): 0.046 M^{-1} h^{-1} (aq) and 0.10 M^{-1} h^{-1} (MeOH).

DOI: 10.1021/acs.jpclett.6b02969
J. Phys. Chem. Lett. 2017, 8, 1503−1511

sulfate) was one of the processes by which the relatively volatile alkylamines were contributing to the particle phase. Alkylamines have been shown to contribute up to 20% of particle-phase organic mass,[47] with some contribution from organic salt formation and some from oxidation.[48] More recent ambient measurements show strong correlations between particle-phase dimethylamine, sulfate, and particle-phase water, supporting the role of organic salt formation for SOA mass growth.[49] In addition to SOA mass growth, organic salt formation may play a role in the nucleation and growth of new particles in the atmosphere.[50−53] Low-volatility organosulfates, products of accretion reactions between epoxides and hydroperoxides formed in acidic sulfate particles, have been detected using online and offline techniques in laboratory and ambient OA particles (e.g., refs 54 and 55).

Given that multiphase accretion product and organic salt formation lead to vapor pressures that are far lower than that of the parent compounds and that the products of such reactions may be detected as monomer decomposition products, there is a critical need for unified predictions of product formation and subsequent partitioning to the particle phase. The gas-particle partitioning of closed-shell monomer reactants and products of accretion and organic salt reactions can be represented in an equilibrium modeling framework, as illustrated in Figure 3. This

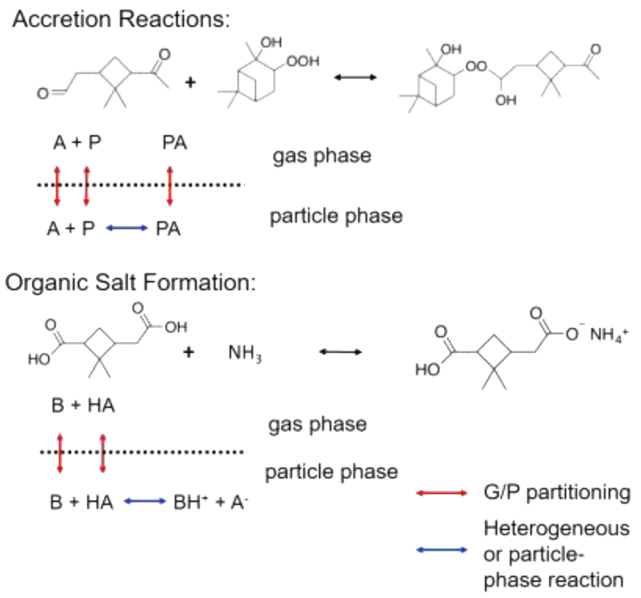

Figure 3. Schematic of the thermodynamic equilibrium framework for representing accretion products and organic salts according to eq 1. The partitioning of the monomers to the particle phase can be represented by an effective volatility that accounts for the extent of product formation. This is given by eq 3 for accretion products and eqs 5 and 7 for organic salts. Alternatively the monomers and dimers can be represented explicitly. In either case, the extent of product formation must be known or approximated to capture the effective volatility of the monomeric compounds.

approach requires knowledge of: (1) the (effective) volatility of the product and (2) the extent of reaction (e.g., Gibbs free energies for accretion reactions or the extent of ionization for organic salt formation).[56,57] For accretion reactions, the computationally derived free energies for selected accretion products (included in DePalma et al.[45]) are compiled in Table 1. To quantitatively describe the differential contribution of monomers versus accretion products to SOA formation, the c^* values and the particle-phase fractions ($f_{p,i} = (1 + c_i^*/M_{OA})^{-1}$) as a function of OA mass (M_{OA}) are listed in Table 2 for the accretion reactions considered by DePalma et al. and those in Figure 1.

The effective volatility associated with accretion product formation can be represented by first determining a mass-weighted average particle-phase fraction ($\overline{f_p}$) for the reactants and product of a single reaction

$$\overline{f}_p = \sum_j \overline{m}_j^* f_{p,j} \tag{2}$$

where the mass fraction, $\overline{m}_j$, is the ratio of the mass of each reactant (monomer) and product (dimer or higher order oligomer) j to the total mass of reactants + product for the reaction of interest. Then, from $\overline{f}_p$, eq 3 (a derivation of eq 1) can be solved for the effective saturation vapor concentration (c_{eff}^*) as a function of M_{OA}

$$\overline{f}_p = (1 + c_{eff}^*/M_{OA})^{-1} \tag{3}$$

Nonequilibrium values can be used in eqs 2 and 3 to obtain time-dependent calculations of c_{eff}^* as a function of M_{OA}. In Figure 4, values of c_{eff}^* associated with peroxyhemiacetal formation are shown for M_{OA} = 1, 10, and 50 μg m^{-3} as a function of the extent of peroxyhemiacetal formation (represented as the mass fraction of peroxyhemiacetal formed). For illustrative purposes, the mass fraction of peroxyhemiacetal was assigned values between 0 and 0.9. In the atmosphere, at thermodynamic equilibrium the extent of accretion product formation will depend on the concentration of the monomers, the equilibrium constant of reaction, the volatility of the monomers and dimers (or higher order oligomers), and the ambient OA concentration.[7] For the peroxyhemiacetal illustrated in Figure 1, the norpinonaldehyde monomer is volatile and contributes negligibly to SOA at all M_{OA}; however, for the hydroperoxide monomer, f_p = 0.03 at M_{OA} = 10 μg m^{-3} and f_p = 0.14 at M_{OA} = 50 μg m^{-3} (see Table 2). When the mass fraction of the peroxyhemiacetal dimer = 0.10, $\overline{f}_p$ = 0.10 at all M_{OA}. As illustrated in Figure 4, the c_{eff}^* values shift from the volatile to semivolatile range when the mass fraction of peroxyhemiacetal is between ∼0.1 and 1% (M_{OA} = 1 μg m^{-3}), ∼1 and 10% (M_{OA} = 10 μg m^{-3}), and 10 and 20% (M_{OA} = 50 μg m^{-3}). For M_{OA} = 1 μg m^{-3}, the c_{eff}^* values shift from the semivolatile to low-volatility range when the mass fraction of peroxyhemiacetal is ∼0.8.

The effective volatility due to organic salt formation can be expressed as a function of the extent to which a given acid or base exists in its ionized form. As in Pankow,[7] the fraction of acid A that is in the neutral form is given by

$$\alpha_0 = \frac{\{HA\}}{\{HA\} + \{A^-\}} = \frac{\{H^+\}}{\{H^+\} + K_a} \tag{4}$$

where {HA} and {A$^-$} are the activity-corrected concentrations of the acid in the neutral and ionized forms, respectively, {H$^+$} is the activity-corrected concentration of hydrogen ion (determinable by pH), and K_a is the acid dissociation constant. The effective saturation concentration (c_{eff}^*) is then the product of the c^* value for the neutral compound and the fraction in the neutral form[5]

DOI: 10.1021/acs.jpclett.6b02969
J. Phys. Chem. Lett. 2017, 8, 1503−1511

Table 2. Saturation Concentrations (c^* in $\mu g\ m^{-3}$) and Particle-Phase Fractions (f_p) of Selected Autoxidation and Accretion Products[a]

		c^*	f_p @ M_{OA} = 1 ug m^{-3}	f_p @ M_{OA} = 10 ug m^{-3}	f_p @ M_{OA} = 50 ug m^{-3}
DePalma et al.	peroxyhemiacetal (PA)	2.3×10^{-4}	1.00	1.00	1.00
	PA monomer	5.4×10^{3}	0.00	0.00	0.02
	hemiacetal (HA)	1.9×10^{-6}	1.00	1.00	1.00
	HA monomer 1	3.8×10^{0}	0.21	0.73	0.93
	HA monomer 2	1.8×10^{5}	0.00	0.00	0.00
	esterification (E)	4.5×10^{-5}	1.00	1.00	1.00
	E monomer 1	5.9×10^{1}	0.02	0.15	0.46
	E monomer 2	1.6×10^{1}	0.06	0.38	0.75
	aldol addition (AA)	8.2×10^{-6}	1.00	1.00	1.00
	AA monomer 1	1.8×10^{5}	0.00	0.00	0.00
	AA monomer 2	6.6×10^{2}	0.00	0.02	0.13
this work	peroxyhemiacetal	5.3×10^{-4}	1.00	1.00	1.00
	norpinonaldehyde	1.8×10^{5}	0.00	0.00	0.00
	hydroperoxide	3.1×10^{2}	0.00	0.03	0.14
	autoxidation monomer	4.4×10^{-4}	1.00	1.00	1.00
	autoxidation dimer	5.7×10^{-9}	1.00	1.00	1.00

[a]Values of c^* calculated using vapor pressures based on the SIMPOL group contribution method of Pankow and Asher.[58]

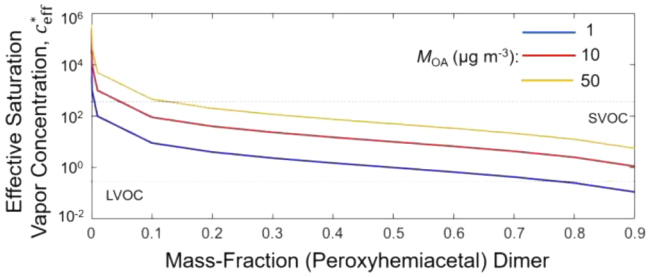

Figure 4. Effective saturation vapor concentration (c^*_{eff}, log scale) for accretion product (peroxyhemiacetal, Figure 1) formation as a function of the extent of reaction (represented by the mass-fraction of peroxyhemiacetal formed) and organic aerosol mass concentration (M_{OA}).

$$c^*_{HA,eff} = c^*_{HA} * \frac{\{H^+\}}{\{H^+\} + K_a} \quad (5)$$

The equivalent expressions for bases are as follows

$$\alpha_1 = \frac{\{B\}}{\{B\} + \{BH^+\}} = \frac{K_a}{\{H^+\} + K_a} \quad (6)$$

$$c^*_{B,eff} = c^*_{B} * \frac{K_a}{\{H^+\} + K_a} \quad (7)$$

where the fraction of base B in the neutral form is given by α_1 and $\{B\}$ and $\{BH^+\}$ are the activity-corrected concentrations of the base in the neutral and ionized forms, respectively. In Figure 5, calculated $c^*_{HA,eff}$ values are shown as a function of pH (0 to 5) for representative organic acid pK_a values: 1.26 (oxalic), 3.75 (formic), and 4.76 (pinic). For figure clarity, only $c^*_{HA,eff}$ for c^*_{HA} = 10^3 and 10^{-3} are shown. In general, as pH increases the fraction of organic acid that is in the ionized form increases, thereby decreasing $c^*_{HA,eff}$. Atmospheric particles typically are acidic, with reported pH values from −0.5 and 3.[59,60] Between pH values of 1 and 3, only the most acidic organic acids (p$K_a \approx 1.26$) would have a fraction of acid in the ionized form (Figure 5); the ionized fraction is >0.5 at pH ≥ 1.25, and at pH 3, the calculated $c^*_{HA,eff}$ is ∼2 orders of magnitude less than c^*_{HA}. The other two organic acids (p$K_a \approx$ 3.75 and 4.76) exhibit little to no dissociation at pH <4, and thus $c^*_{HA,eff} \cong c^*_{HA}$. Atmospheric organic bases, with pK_a values ∼9 to 11, would exist largely in the ionized form and thus would be essentially nonvolatile in acidic particles.

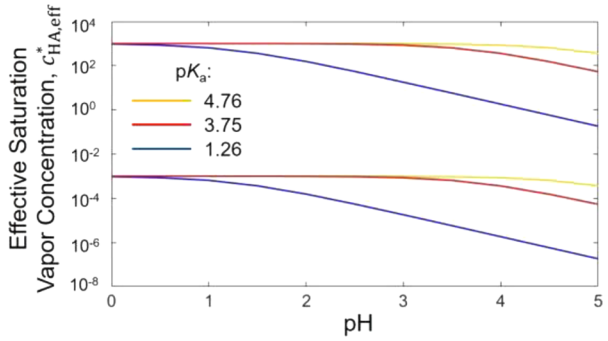

Figure 5. Organic acid effective saturation concentration ($c^*_{HA,eff}$, log scale) as a function of pH; neutral-compound c^* values of 10^{-3} and 10^3 are shown for representative organic acid pK_a values of 1.26 (blue), 3.75 (red), and 4.76 (blue). The value of $c^*_{HA,eff}$ decreases as pH increases and the ionized (nonvolatile) fraction of the acid increases.

While a partitioning-based framework for estimating the effective volatility of (E)LVOCs (and their contributions to

While a partitioning-based framework for estimating the effective volatility of (E)LVOCs (and their contributions to SOA formation) is provided, the utility of that framework for ambient predictions is dependent on our understanding of the molecular-level chemistry of atmospherically relevant reactions and products, which remains quite limited.

DOI: 10.1021/acs.jpclett.6b02969
J. Phys. Chem. Lett. 2017, 8, 1503−1511

SOA formation) is provided, the utility of that framework for ambient predictions is dependent on our understanding of the molecular-level chemistry of atmospherically relevant reactions and products, which remains quite limited. Analytical methods that approach mass closure (e.g., HR-ToF-CIMS) are unable to distinguish molecular isomers or yet provide structural information, while those that are able to speciate isomers (e.g., SV-TAG) may be sensitive to only a small fraction of the condensed phase species. Moreover, the techniques capable of quantification often involve thermal desorption, which does not necessarily preserve molecular structures of condensed-phase compounds. While it now seems likely that the processes described herein play an important role in new particle formation and SOA mass growth, important issues remain unresolved.

With regard to autoxidation, the absolute yields of highly oxygenated (E)LVOCs from various combinations of oxidants and hydrocarbons remain uncertain or relatively unexplored under the range of atmospherically relevant conditions (e.g., oxidant and precursor levels, and T). The mechanism(s) forming highly oxidized gas-phase dimers remains largely unknown, as do the relative yields of the dimers over a wide range of ambient conditions. The c^* values of the resultant highly oxygenated (E)LVOC monomers and dimers, while expected to be sufficiently low (at least from monoterpene oxidation), remain only calculated from group contribution methods or indirectly inferred from thermal desorption,[29] approaches that have significant uncertainties when applied to highly oxygenated molecules.[61] Finally, given the numerous −OOH groups, these autoxidation products are highly reactive and hence well-suited to participate in multiphase reactions; the effects of such reactions on SOA formation and lifetime remain necessary to assess. With regard to accretion reactions, experimental constraints on the kinetics and thermodynamics of the formation and lifetime of dimers and higher-order products are lacking, particularly spanning the full range of atmospherically relevant conditions (e.g., oxidant levels, gas and particle composition, T, and RH). Reactions forming accretion products are likely to be nonlinear in precursor concentrations, and thus accurate simulation in the laboratory will require careful attention to the concentration regimes of the precursors and radicals involved in the oxidation process and environmental conditions such as temperature and humidity.[62] Whether there are specific VOC precursors that form accretion products more readily than others or if accretion is a general feature of SOA formation remains to be determined. Furthermore, the identities and quantities of the gas-phase oxidation products that might participate in atmospheric accretion reactions are not well known. Finally, presumably there is a connection between the extent of oligomerization and particle viscosity,[63] which would, in turn, affect the efficiency of heterogeneous and bulk-phase reactions.

Further insights into the chemical and physical properties of atmospheric SOA are expected, with continuing and rapid advances in analytical approaches. Techniques like particle evaporation studies coupled to online composition measurements and methods that do not induce thermal decomposition will allow better estimates of the mass contribution of oligomers as a function of precursor concentration and the rate or extent of their decomposition. Moreover, increased use of techniques capable of revealing chemical structures (e.g., ion mobility and MS^n) will allow more complete mechanistic understanding and more refined computational studies to develop quantitative estimates of reaction and partitioning kinetics and thermodynamics. Such studies will improve the utility of the thermodynamic framework for the prediction of SOA formation by autoxidation, accretion, and organic salt reactions and thus facilitate more accurate projections of air quality and climate conditions affected by SOA.

Further insights into the chemical and physical properties of atmospheric SOA are expected, with continuing and rapid advances in analytical approaches.

AUTHOR INFORMATION

Corresponding Author

*E-mail: kbarsanti@engr.ucr.edu.

ORCID

Kelley C. Barsanti: 0000-0002-6065-8643

Notes

The authors declare no competing financial interest.

ACKNOWLEDGMENTS

K.C.B. was supported through an award from the Bureau of Land Management Joint Fire Science Program (14-1-03-44). J.H.K. was supported the National Science Foundation through awards from Atmospheric and Geospace Sciences (AGS-1536551, AGS-1638672). J.A.T. was supported by the U.S. Department of Energy through an award from the Atmospheric System Research Program (DOE Grant DE-SC0006867).

REFERENCES

(1) Jimenez, J. L.; Canagaratna, M. R.; Donahue, N. M.; Prevot, A. S. H.; Zhang, Q.; Kroll, J. H.; DeCarlo, P. F.; Allan, J. D.; Coe, H.; Ng, N. L.; et al. Evolution of Organic Aerosols in the Atmosphere. *Science* **2009**, *326* (5959), 1525−1529.

(2) Zhang, H. F.; Worton, D. R.; Shen, S.; Nah, T.; Isaacman-VanWertz, G.; Wilson, K. R.; Goldstein, A. H. Fundamental Time Scales Governing Organic Aerosol Multiphase Partitioning and Oxidative Aging. *Environ. Sci. Technol.* **2015**, *49* (16), 9768−9777.

(3) Kroll, J. H.; Seinfeld, J. H. Chemistry of secondary organic aerosol: Formation and evolution of low-volatility organics in the atmosphere. *Atmos. Environ.* **2008**, *42* (16), 3593−3624.

(4) Pankow, J. F. An absorption model of gas-particle partitioning of organic compounds in the atmosphere. *Atmos. Environ.* **1994**, *28* (2), 185−188.

(5) Odum, J. R.; Jungkamp, T. P. W.; Griffin, R. J.; Forstner, H. J. L.; Flagan, R. C.; Seinfeld, J. H. Aromatics, reformulated gasoline, and atmospheric organic aerosol formation. *Environ. Sci. Technol.* **1997**, *31* (7), 1890−1897.

(6) Donahue, N. M.; Robinson, A. L.; Stanier, C. O.; Pandis, S. N. Coupled partitioning, dilution, and chemical aging of semivolatile organics. *Environ. Sci. Technol.* **2006**, *40* (8), 2635−2643.

(7) Pankow, J. F. Gas/particle partitioning of neutral and ionizing compounds to single and multi-phase aerosol particles. 1. Unified modeling framework. *Atmos. Environ.* **2003**, *37* (24), 3323−3333.

(8) Pankow, J. F.; Marks, M. C.; Barsanti, K. C.; Mahmud, A.; Asher, W. E.; Li, J. Y.; Ying, Q.; Jathar, S. H.; Kleeman, M. J. Molecular view modeling of atmospheric organic particulate matter: Incorporating molecular structure and co-condensation of water. *Atmos. Environ.* **2015**, *122*, 400−408.

DOI: 10.1021/acs.jpclett.6b02969
J. Phys. Chem. Lett. 2017, 8, 1503−1511

(9) Shiraiwa, M.; Seinfeld, J. H. Equilibration timescale of atmospheric secondary organic aerosol partitioning. *Geophys. Res. Lett.* **2012**, *39*, L24801.
(10) Perraud, V.; Bruns, E. A.; Ezell, M. J.; Johnson, S. N.; Yu, Y.; Alexander, M. L.; Zelenyuk, A.; Imre, D.; Chang, W. L.; Dabdub, D.; et al. Nonequilibrium atmospheric secondary organic aerosol formation and growth. *Proc. Natl. Acad. Sci. U. S. A.* **2012**, *109* (8), 2836−2841.
(11) Liu, P. F.; Li, Y. J.; Wang, Y.; Gilles, M. K.; Zaveri, R. A.; Bertram, A. K.; Martin, S. T. Lability of secondary organic particulate matter. *Proc. Natl. Acad. Sci. U. S. A.* **2016**, *113* (45), 12643−12648.
(12) Barsanti, K. C.; Pankow, J. F. Thermodynamics of the formation of atmospheric organic particulate matter by accretion reactions - Part 1: Aldehydes and ketones. *Atmos. Environ.* **2004**, *38* (26), 4371−4382.
(13) Hallquist, M.; Wenger, J. C.; Baltensperger, U.; Rudich, Y.; Simpson, D.; Claeys, M.; Dommen, J.; Donahue, N. M.; George, C.; Goldstein, A. H.; et al. The formation, properties and impact of secondary organic aerosol: current and emerging issues. *Atmos. Chem. Phys.* **2009**, *9* (14), 5155−5236.
(14) Ziemann, P. J.; Atkinson, R. Kinetics, products, and mechanisms of secondary organic aerosol formation. *Chem. Soc. Rev.* **2012**, *41* (19), 6582−6605.
(15) Donahue, N. M.; Kroll, J. H.; Pandis, S. N.; Robinson, A. L. A two-dimensional volatility basis set − Part 2: Diagnostics of organic-aerosol evolution. *Atmos. Chem. Phys.* **2012**, *12* (2), 615−634.
(16) Kurtén, T.; Rissanen, M. P.; Mackeprang, K.; Thornton, J. A.; Hyttinen, N.; Jørgensen, S.; Ehn, M.; Kjaergaard, H. G. Computational Study of Hydrogen Shifts and Ring-Opening Mechanisms in α-Pinene Ozonolysis Products. *J. Phys. Chem. A* **2015**, *119* (46), 11366−11375.
(17) Crounse, J. D.; Paulot, F.; Kjaergaard, H. G.; Wennberg, P. O. Peroxy radical isomerization in the oxidation of isoprene. *Phys. Chem. Chem. Phys.* **2011**, *13* (30), 13607−13613.
(18) Ehn, M.; Thornton, J. A.; Kleist, E.; Sipila, M.; Junninen, H.; Pullinen, I.; Springer, M.; Rubach, F.; Tillmann, R.; Lee, B.; et al. A large source of low-volatility secondary organic aerosol. *Nature* **2014**, *506* (7489), 476−479.
(19) Elm, J.; Myllys, N.; Hyttinen, N.; Kurten, T. Computational study of the clustering of a cyclohexene autoxidation product C6H8O7 with itself and sulfuric acid. *J. Phys. Chem. A* **2015**, *119* (30), 8414−8421.
(20) Rissanen, M. P.; Kurten, T.; Sipila, M.; Thornton, J. A.; Kausiala, O.; Garmash, O.; Kjaergaard, H. G.; Petaja, T.; Worsnop, D. R.; Ehn, M.; et al. Effects of chemical complexity on the autoxidation mechanisms of endocyclic alkene ozonolysis products: From methylcyclohexenes toward understanding alpha-pinene. *J. Phys. Chem. A* **2015**, *119* (19), 4633−4650.
(21) Bonner, B. H.; Tipper, C. F. H. The cool flame combustion of hydrocarbons II—Propane and n-heptane. *Combust. Flame* **1965**, *9* (4), 387−392.
(22) Barnard, J. A.; Harwood, B. A. Slow combustion and cool-flame behavior of iso-octane. *Combust. Flame* **1973**, *21* (3), 345−355.
(23) Crounse, J. D.; Nielsen, L. B.; Jorgensen, S.; Kjaergaard, H. G.; Wennberg, P. O. Autoxidation of organic compounds in the atmosphere. *J. Phys. Chem. Lett.* **2013**, *4* (20), 3513−3520.
(24) Peeters, J.; Nguyen, T. L.; Vereecken, L. HOx radical regeneration in the oxidation of isoprene. *Phys. Chem. Chem. Phys.* **2009**, *11* (28), 5935−5939.
(25) Da Silva, G.; Graham, C.; Wang, Z.-F. Unimolecular beta-hydroxyperoxy radical decomposition with OH recycling in the photochemical oxidation of isoprene. *Environ. Sci. Technol.* **2010**, *44* (1), 250−256.
(26) St. Clair, J. M.; Rivera-Rios, J. C.; Crounse, J. D.; Knap, H. C.; Bates, K. H.; Teng, A. P.; Jorgensen, S.; Kjaergaard, H. G.; Keutsch, F. N.; Wennberg, P. O. Kinetics and products of the reaction of the first-generation isoprene hydroxy hydroperoxide (ISOPOOH) with OH. *J. Phys. Chem. A* **2016**, *120* (9), 1441−1451.
(27) Ehn, M.; Kleist, E.; Junninen, H.; Petaja, T.; Lonn, G.; Schobesberger, S.; Dal Maso, M.; Trimborn, A.; Kulmala, M.; Worsnop, D. R.; et al. Gas phase formation of extremely oxidized pinene reaction products in chamber and ambient air. *Atmos. Chem. Phys.* **2012**, *12* (11), 5113−5127.
(28) Jokinen, T.; Berndt, T.; Makkonen, R.; Kerminen, V. M.; Junninen, H.; Paasonen, P.; Stratmann, F.; Herrmann, H.; Guenther, A. B.; Worsnop, D. R.; et al. Production of extremely low volatile organic compounds from biogenic emissions: Measured yields and atmospheric implications. *Proc. Natl. Acad. Sci. U. S. A.* **2015**, *112* (23), 7123−7128.
(29) Lopez-Hilfiker, F. D.; Mohr, C.; Ehn, M.; Rubach, F.; Kleist, E.; Wildt, J.; Mentel, T. F.; Lutz, A.; Hallquist, M.; Worsnop, D.; et al. A novel method for online analysis of gas and particle composition: description and evaluation of a Filter Inlet for Gases and AEROsols (FIGAERO). *Atmos. Meas. Tech.* **2014**, *7* (4), 983−1001.
(30) Trostl, J.; Chuang, W. K.; Gordon, H.; Heinritzi, M.; Yan, C.; Molteni, U.; Ahlm, L.; Frege, C.; Bianchi, F.; Wagner, R.; et al. The role of low-volatility organic compounds in initial particle growth in the atmosphere. *Nature* **2016**, *533* (7604), 527−531.
(31) Kundu, S.; Fisseha, R.; Putman, A. L.; Rahn, T. A.; Mazzoleni, L. R. High molecular weight SOA formation during limonene ozonolysis: insights from ultrahigh-resolution FT-ICR mass spectrometry characterization. *Atmos. Chem. Phys.* **2012**, *12* (12), 5523−5536.
(32) Tobias, H. J.; Ziemann, P. J. Compound identification in organic aerosols using temperature-programmed thermal desorption particle beam mass spectrometry. *Anal. Chem.* **1999**, *71* (16), 3428−3435.
(33) Tobias, H. J.; Ziemann, P. J. Kinetics of the gas-phase reactions of alcohols, aldehydes, carboxylic acids, and water with the C13 stabilized Criegee intermediate formed from ozonolysis of 1-tetradecene. *J. Phys. Chem. A* **2001**, *105* (25), 6129−6135.
(34) Jang, M. S.; Kamens, R. M. Atmospheric secondary aerosol formation by heterogeneous reactions of aldehydes in the presence of a sulfuric acid aerosol catalyst. *Environ. Sci. Technol.* **2001**, *35* (24), 4758−4766.
(35) Lopez-Hilfiker, F. D.; Mohr, C.; Ehn, M.; Rubach, F.; Kleist, E.; Wildt, J.; Mentel, T. F.; Carrasquillo, A. J.; Daumit, K. E.; Hunter, J. F.; et al. Phase partitioning and volatility of secondary organic aerosol components formed from alpha-pinene ozonolysis and OH oxidation: the importance of accretion products and other low volatility compounds. *Atmos. Chem. Phys.* **2015**, *15* (14), 7765−7776.
(36) Williams, B. J.; Goldstein, A. H.; Kreisberg, N. M.; Hering, S. V. In situ measurements of gas/particle-phase transitions for atmospheric semivolatile organic compounds. *Proc. Natl. Acad. Sci. U. S. A.* **2010**, *107* (15), 6676−6681.
(37) Isaacman-VanWertz, G.; Yee, L. D.; Kreisberg, N. M.; Wernis, R.; Moss, J. A.; Hering, S. V.; de Sa, S. S.; Martin, S. T.; Alexander, M. L.; Palm, B. B.; et al. Ambient gas-particle partitioning of tracers for biogenic oxidation. *Environ. Sci. Technol.* **2016**, *50* (18), 9952−9962.
(38) Bahreini, R.; Keywood, M. D.; Ng, N. L.; Varutbangkul, V.; Gao, S.; Flagan, R. C.; Seinfeld, J. H.; Worsnop, D. R.; Jimenez, J. L. Measurements of secondary organic aerosol from oxidation of cycloalkenes, terpenes, and m-xylene using an Aerodyne aerosol mass spectrometer. *Environ. Sci. Technol.* **2005**, *39* (15), 5674−5688.
(39) Kroll, J. H.; Ng, N. L.; Murphy, S. M.; Flagan, R. C.; Seinfeld, J. H. Secondary organic aerosol formation from isoprene photooxidation. *Environ. Sci. Technol.* **2006**, *40* (6), 1869−1877.
(40) Tolocka, M. P.; Jang, M.; Ginter, J. M.; Cox, F. J.; Kamens, R. M.; Johnston, M. V. Formation of oligomers in secondary organic aerosol. *Environ. Sci. Technol.* **2004**, *38* (5), 1428−1434.
(41) Kalberer, M.; Paulsen, D.; Sax, M.; Steinbacher, M.; Dommen, J.; Prevot, A. S. H.; Fisseha, R.; Weingartner, E.; Frankevich, V.; Zenobi, R.; et al. Identification of polymers as major components of atmospheric organic aerosols. *Science* **2004**, *303* (5664), 1659−1662.
(42) Hall, W. A.; Johnston, M. V. Oligomer formation pathways in secondary organic aerosol from MS and MS/MS measurements with high mass accuracy and resolving power. *J. Am. Soc. Mass Spectrom.* **2012**, *23* (6), 1097−1108.
(43) Barsanti, K. C.; Pankow, J. F. Thermodynamics of the formation of atmospheric organic particulate matter by accretion reactions - Part 3: Carboxylic and dicarboxylic acids. *Atmos. Environ.* **2006**, *40* (34), 6676−6686.

DOI: 10.1021/acs.jpclett.6b02969
J. Phys. Chem. Lett. 2017, 8, 1503−1511

(44) Tong, C. H.; Blanco, M.; Goddard, W. A.; Seinfeld, J. H. Secondary organic aerosol formation by heterogeneous reactions of aldehydes and ketones: A quantum mechanical study. *Environ. Sci. Technol.* **2006**, *40* (7), 2333−2338.
(45) DePalma, J. W.; Horan, A. J.; Hall, W. A., IV; Johnston, M. V. Thermodynamics of oligomer formation: implications for secondary organic aerosol formation and reactivity. *Phys. Chem. Chem. Phys.* **2013**, *15* (18), 6935−6944.
(46) Angelino, S.; Suess, D. T.; Prather, K. A. Formation of aerosol particles from reactions of secondary and tertiary alkylamines: Characterization by aerosol time-of-flight mass spectrometry. *Environ. Sci. Technol.* **2001**, *35* (15), 3130−3138.
(47) Silva, P. J.; Erupe, M. E.; Price, D.; Elias, J.; Malloy, Q. G. J.; Li, Q.; Warren, B.; Cocker, D. R. Trimethylamine as precursor to secondary organic aerosol formation via nitrate radical reaction in the atmosphere. *Environ. Sci. Technol.* **2008**, *42* (13), 4689−4696.
(48) Price, D. J.; Clark, C. H.; Tang, X. C.; Cocker, D. R.; Purvis-Roberts, K. L.; Silva, P. J. Proposed chemical mechanisms leading to secondary organic aerosol in the reactions of aliphatic amines with hydroxyl and nitrate radicals. *Atmos. Environ.* **2014**, *96*, 135−144.
(49) Youn, J. S.; Crosbie, E.; Maudlin, L. C.; Wang, Z.; Sorooshian, A. Dimethylamine as a major alkyl amine species in particles and cloud water: Observations in semi-arid and coastal regions. *Atmos. Environ.* **2015**, *122*, 250−258.
(50) Smith, J. N.; Barsanti, K. C.; Friedli, H. R.; Ehn, M.; Kulmala, M.; Collins, D. R.; Scheckman, J. H.; Williams, B. J.; McMurry, P. H. Observations of aminium salts in atmospheric nanoparticles and possible climatic implications. *Proc. Natl. Acad. Sci. U. S. A.* **2010**, *107* (15), 6634−6639.
(51) Riipinen, I.; Pierce, J. R.; Yli-Juuti, T.; Nieminen, T.; Hakkinen, S.; Ehn, M.; Junninen, H.; Lehtipalo, K.; Petaja, T.; Slowik, J.; et al. Organic condensation: a vital link connecting aerosol formation to cloud condensation nuclei (CCN) concentrations. *Atmos. Chem. Phys.* **2011**, *11* (8), 3865−3878.
(52) Mackenzie, R. B.; Dewberry, C. T.; Leopold, K. R. The trimethylamine-formic acid complex: Microwave characterization of a prototype for potential precursors to atmospheric aerosol. *J. Phys. Chem. A* **2016**, *120* (14), 2268−2273.
(53) Almeida, J.; Schobesberger, S.; Kurten, A.; Ortega, I. K.; Kupiainen-Maatta, O.; Praplan, A. P.; Adamov, A.; Amorim, A.; Bianchi, F.; Breitenlechner, M.; et al. Molecular understanding of sulphuric acid-amine particle nucleation in the atmosphere. *Nature* **2013**, *502* (7471), 359−363.
(54) Surratt, J. D.; Gomez-Gonzalez, Y.; Chan, A. W. H.; Vermeylen, R.; Shahgholi, M.; Kleindienst, T. E.; Edney, E. O.; Offenberg, J. H.; Lewandowski, M.; Jaoui, M.; et al. Organosulfate formation in biogenic secondary organic aerosol. *J. Phys. Chem. A* **2008**, *112* (36), 8345−8378.
(55) Hatch, L. E.; Creamean, J. M.; Ault, A. P.; Surratt, J. D.; Chan, M. N.; Seinfeld, J. H.; Edgerton, E. S.; Su, Y. X.; Prather, K. A. Measurements of isoprene-derived organosulfates in ambient aerosols by aerosol time-of-flight mass spectrometry - Part 1: Single particle atmospheric observations in Atlanta. *Environ. Sci. Technol.* **2011**, *45* (12), 5105−5111.
(56) Kroll, J. H.; Seinfeld, J. H. Representation of secondary organic aerosol laboratory chamber data for the interpretation of mechanisms of particle growth. *Environ. Sci. Technol.* **2005**, *39* (11), 4159−4165.
(57) Trump, E. R.; Donahue, N. M. Oligomer formation within secondary organic aerosols: equilibrium and dynamic considerations. *Atmos. Chem. Phys.* **2014**, *14* (7), 3691−3701.
(58) Pankow, J. F.; Asher, W. E. SIMPOL.1: A simple group contribution method for predicting vapor pressures and enthalpies of vaporization of multifunctional organic compounds. *Atmos. Chem. Phys.* **2008**, *8* (10), 2773−2796.
(59) Guo, H.; Xu, L.; Bougiatioti, A.; Cerully, K. M.; Capps, S. L.; Hite, J. R.; Carlton, A. G.; Lee, S. H.; Bergin, M. H.; Ng, N. L.; et al. Fine-particle water and pH in the southeastern United States. *Atmos. Chem. Phys.* **2015**, *15* (9), 5211−5228.
(60) Guo, H.; Sullivan, A. P.; Campuzano-Jost, P.; Schroder, J. C.; Lopez-Hilfiker, F. D.; Dibb, J. E.; Jimenez, J. L.; Thornton, J. A.; Brown, S. S.; Nenes, A.; et al. Fine particle pH and the partitioning of nitric acid during winter in the northeastern United States. *J. Geophys. Res.: Atmos.* **2016**, *121* (17), 10,355−10,376.
(61) Kurten, T.; Tiusanen, K.; Roldin, P.; Rissanen, M.; Luy, J. N.; Boy, M.; Ehn, M.; Donahue, N. M. Alpha-pinene autoxidation products may not have extremely low saturation vapor pressures despite high O:C ratios. *J. Phys. Chem. A* **2016**, *120* (16), 2569−2582.
(62) Kourtchev, I.; Giorio, C.; Manninen, A.; Wilson, E.; Mahon, B.; Aalto, J.; Kajos, M.; Venables, D.; Ruuskanen, T.; Levula, J.; et al. Enhanced volatile organic compounds emissions and organic aerosol mass increase the oligomer content of atmospheric aerosols. *Sci. Rep.* **2016**, *6*, 35038.
(63) Kidd, C.; Perraud, V.; Wingen, L. M.; Finlayson-Pitts, B. J. Integrating phase and composition of secondary organic aerosol from the ozonolysis of α-pinene. *Proc. Natl. Acad. Sci. U. S. A.* **2014**, *111* (21), 7552−7557.

DOI: 10.1021/acs.jpclett.6b02969
J. Phys. Chem. Lett. 2017, 8, 1503−1511